

Current-induced nonlinear conduction of two-electron doped manganites $\text{Ca}_{1-x}\text{Ce}_x\text{MnO}_3$

Y Yamato¹, M Matsukawa¹, Y Murano¹, S Kobayashi¹ and R Suryanarayanan²

¹ Department of Materials Science and Engineering, Iwate University, Morioka 020-8551, Japan

² Laboratoire de Physico-Chimie de L'Etat Solide, CNRS, UMR8182 Universite Paris-Sud, 91405 Orsay, France

Received 7 January 2010, in final form 25 February 2010

Published 23 March 2010

Online at stacks.iop.org/JPhysD/43/145003

Abstract

We have investigated the current-induced nonlinear conduction in a charge-ordered phase of two-electron doped manganites $\text{Ca}_{1-x}\text{Ce}_x\text{MnO}_3$ ($x = 0.1$ and 0.167). The substitution of Ce^{4+} ion for Ca^{2+} site of the parent matrix causes two-electron doping with the chemical formula $\text{Ca}_{1-x}^{2+}\text{Ce}_x^{4+}\text{Mn}_{1-2x}^{4+}\text{Mn}_{2x}^{3+}\text{O}_3$. Seebeck coefficient data of $\text{Ca}_{0.9}\text{Ce}_{0.1}\text{MnO}_3$ are, in both its temperature dependence and its magnitude, very similar to those of $\text{Ca}_{0.8}\text{Sm}_{0.2}\text{MnO}_3$, leading to further evidence for two-electron doping. The VI characteristics measured using a long pulsed current show a negative differential resistance and its associated giant electroresistance effect. It is demonstrated that a temperature rise across the samples due to Joule heating is not responsible for a huge decrease in resistance observed here.

(Some figures in this article are in colour only in the electronic version)

1. Introduction

Perovskite manganites show a large variety of fascinating properties such as the colossal magnetoresistance (CMR) effect and the charge-orbital ordered (CO) insulating phase [1]. The most interesting one is the existence of a phase-separated state, the coexistence of antiferromagnetic (AFM) CO insulating and ferromagnetic metal (FMM) regions [2]. The phenomenon of microscopic phase separation into two competing ordered phases on various length scales has a close relation to quenched disorder existing in doped manganites. Recently, it has been reported that the resistance of CO manganites exhibits a significant change when a strong electric field or current is applied [3, 4]. The electric current induced resistance change results in switching from the charge-ordered insulating to ferromagnetic metallic state. This phenomenon is called the colossal electroresistance (CER) effect, which is analogous to the term of the CMR effect. The effect of electric fields on the CO state of the manganites is an issue of considerable interest not only on the basis of physical phenomena but also from the viewpoint of technological applications. There have been extensive studies on the effect

of an applied electric current/voltage on the resistance of hole doped manganites causing a huge negative ER effect so far [3–13]. However, they have paid little attention to electron doped manganite systems with a high concentration of Mn^{4+} ions [14, 15].

In this paper, we demonstrate current-induced nonlinear conduction in a charge-ordered phase of two-electron doped manganites $\text{Ca}_{1-x}\text{Ce}_x\text{MnO}_3$ ($x = 0.1$ and 0.167). The substitution of Ce^{4+} ion for Ca^{2+} site produces a two-electron doped manganite system with the chemical formula $\text{Ca}_{1-x}^{2+}\text{Ce}_x^{4+}\text{Mn}_{1-2x}^{4+}\text{Mn}_{2x}^{3+}\text{O}_3$. For a single electron doped system, we have $\text{Ca}_{1-y}^{2+}\text{R}_y^{3+}\text{Mn}_{1-y}^{4+}\text{Mn}_y^{3+}\text{O}_3$ ($R =$ trivalent rare-earth ions). It is well known that for $\text{Ca}_{1-y}\text{R}_y\text{MnO}_3$ ($R = \text{Sm, Pr, Nd, Eu, etc}$) the CMR effect appears in a very narrow range of carrier contents [16]. Zeng *et al* showed that $\text{Ca}_{1-x}\text{Ce}_x\text{MnO}_3$ is a two-electron doped CMR system through a scaling ($x = 2y$) of magnetic properties with respect to a single electron doped system [17]. Furthermore, the x-ray absorption spectroscopy result reveals that the formal valence of Ce ion is 4+. In particular, at the $x = 0.167$ composition with the concentration of $\text{Mn}^{3+} = 1/3$, the CO state is more stabilized.

2. Experiment

Polycrystalline $\text{Ca}_{1-x}\text{Ce}_x\text{MnO}_3$ ($x = 0.1$ and 0.167) were synthesized by a standard solid-state reaction method. The starting materials CaO , CeO_2 and Mn_3O_4 with high purities were mixed, and the formed powders were annealed at 1000 – 1200 °C for 24 h with several grindings. The products were finally pressed into pellets, and they were sintered in air at 1450 °C for 24 h. Powder x-ray diffraction patterns showed the samples are almost single phase with an orthorhombic structure ($Pnma$ space group). The lattice parameters of the $x = 0.1$ sample are $a = 5.3261$ Å, $b = 7.4863$ Å and $c = 5.2961$ Å, which is fairly in agreement with a previous work [18]. The cell parameters and the unit cell volume are elongated upon increasing the Ce doping although the ion radius of Ce^{4+} (1.14 Å) is smaller than the value of Ca^{2+} (1.34 Å). The Mn^{4+} ions (0.53 Å) are replaced by Mn^{3+} ions (0.645 Å) with one extra electron, which contributes to the enhanced cell volume. The temperature variation of electrical resistivity was measured with a standard four-probe method. Electrical contacts were prepared with silver paste on a bar-shaped sample (typical dimension $\sim 8 \times 2 \times 2$ mm³). Seebeck coefficient was determined from both a temperature gradient and its associated thermal voltage across the sample when a thermal current is supplied along its longitudinal direction. The VI characteristics measurement was performed with a two-probe method using a Keithley KE2400 source meter, which enables us to monitor voltage on current contact. The sample was mounted on the cold head of a closed type helium cryocooler surrounded by a vacuum cryostat. Measurement of magnetization was carried out by a superconducting quantum interference device magnetometer. A pulsed current with a time duration of 10 ms was applied from 1 up to 50 mA in steps of $\Delta I = 1$ mA to reduce the Joule heating effect. The applied current was switched off for about 10 ms between successive current steps. The temperature gradient generated across the samples was monitored using a differential-type thermocouple of Au+0.07%Fe alloy versus chromel when the applied current was supplied. One junction of the thermocouple lead was set on the top surface of the sample with a GE7031 varnish and the other one was attached at its bottom on the cold end. Under adiabatic conditions, heat flux generated flows from the hot surface at the top of the sample towards its cold end when the applied current is parallel to both surfaces. For comparison, the VI data of the $x = 0.1$ and 0.167 samples dipped in liquid nitrogen were taken using a stationary current.

3. Results and discussion

First of all, we present in figure 1(a) the temperature variation of electrical resistivity ρ of polycrystalline $\text{Ca}_{1-x}\text{Ce}_x\text{MnO}_3$ ($x = 0.1$ and 0.167). The ρ value of the $x = 0.1$ sample remains nearly constant at high temperatures and it then exhibits a rapid increase below 170 K upon decreasing T , suggesting the weakly metallic to charge-ordered insulator transition. The resistivity of the $x = 0.167$ sample also shows a semiconducting behaviour over a wide range of temperatures and a further increase in ρ appears below

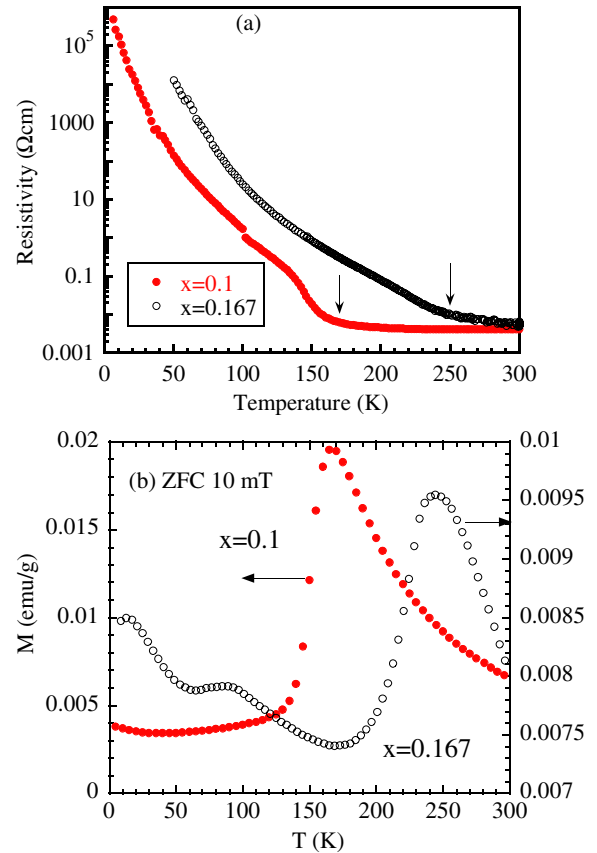


Figure 1. (a) Temperature variation of resistivity ρ of polycrystalline $\text{Ca}_{1-x}\text{Ce}_x\text{MnO}_3$ ($x = 0.1$ and 0.167) measured at a small current of 0.01 mA. Arrows denote the charge-ordered transition temperatures. (b) Temperature variation of zero field cooled (ZFC) magnetization of $\text{Ca}_{1-x}\text{Ce}_x\text{MnO}_3$ ($x = 0.1$ and 0.167) measured under an applied field of 10 mT.

240 K. The magnetization data of the $x = 0.1$ sample, as depicted in figure 1(b), reveal a pronounced peak around 170 K indicating the paramagnetic to AFM transition accompanied by a transition into a charge-ordered insulating state. A similar behaviour on the ZFC run is obtained at $x = 0.167$. Here, we define the charge-ordered insulator transition temperature as T_{CO} . Next, we examine the Seebeck coefficient S of $x = 0.1$ (figure 2), in order to check an electron-doped system of our samples. The value of S shows a monotonic increase down to $T_{\text{CO}} = 170$ K upon cooling the $x = 0.1$ sample and then rapidly starts to drop below T_{CO} . After the value of S reaches a broad minimum around ~ 100 K, at lower temperatures it again begins to exhibit a stable increase crossing the horizontal axis. The Seebeck coefficient is a sensitive probe to examine electronic states of dirty materials since it is less affected by grain boundaries of polycrystalline samples than the resistivity measurement. We note that the S data of $\text{Ca}_{0.9}\text{Ce}_{0.1}\text{MnO}_3$ are, in both its temperature dependence and its magnitude, very similar to those of $\text{Ca}_{0.8}\text{Sm}_{0.2}\text{MnO}_3$, indicating an additional evidence for two-electron doping [19].

Now, let us show the voltage versus current (VI) characteristics of $\text{Ca}_{1-x}\text{Ce}_x\text{MnO}_3$ ($x = 0.1$) at selected temperatures (figure 3(a)). Upon increasing the applied current, at smaller currents the IV data of the $x = 0.1$ sample

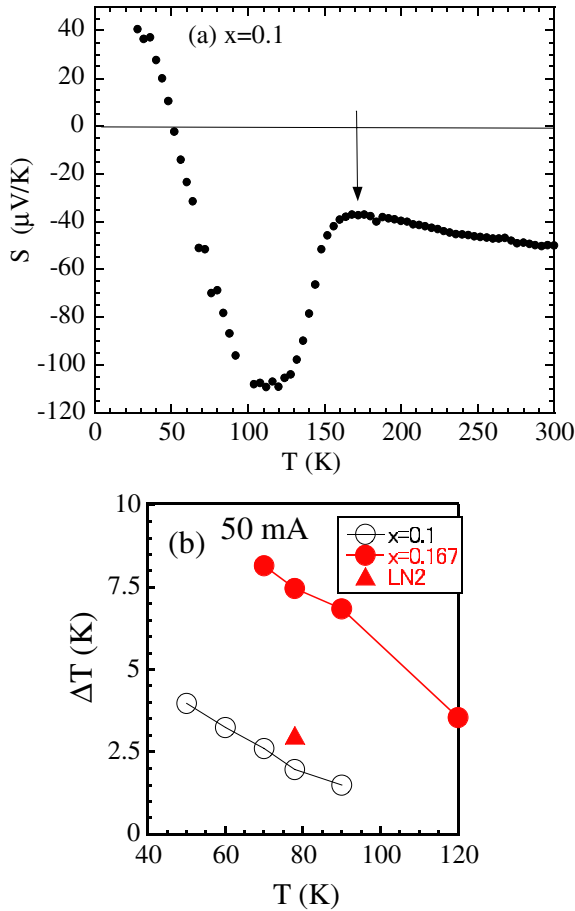


Figure 2. (a) Temperature variation of Seebeck coefficient S of $\text{Ca}_{0.9}\text{Ce}_{0.1}\text{MnO}_3$. The arrow denotes the CO transition temperature. (b) The temperature gradient ΔT generated across the $x = 0.1$ and 0.167 samples at selected temperatures. ΔT is monitored at $I = 50$ mA. For comparison, the temperature rise of the $x = 0.167$ sample dipped in liquid N_2 is given.

follow the Ohmic characteristics and then tend to saturate. As T is lowered below 70 K, a negative differential resistance (NDR) feature occurs at higher currents above a threshold value ranging from 35 mA at 70 K down to 16 mA at 50 K. The current dependence of the corresponding resistance $R = V/I$ follows a strong nonlinearity and the magnitude of R rapidly drops by more than one order of magnitude at higher currents. Figure 3(b) represents the electroresistance ratio (ER) of the $x = 0.1$ sample as a function of applied current. Here, the ER is defined as $[R(I) - R(I_{\text{low}})]/R(I_{\text{low}}) \times 100$, where I_{low} is the lowest current value (1 mA). A giant electroresistance effect reaching ER -90% at $I = 50$ mA for $x = 0.1$ is achieved at 50 K. Our findings are in good agreement with a previous work on the IV data of $\text{Ca}_{1-x}\text{Ce}_x\text{MnO}_3$ ($x = 0.1$) except for the data at LN_2 temperature [14].

To examine the influence of Joule heating on the nonlinear IV characteristics, we check simultaneously a temperature rise of samples studied using differential thermocouples as shown in figure 2. For $x = 0.1$, we obtain $\Delta T = \sim 4$ K ($I = 50$ mA) at 50 K, which never reproduces a huge decrease in R by one order of magnitude. In a similar way, we display in figure 4 the IV characteristics and the ER ratio in the charge-ordered state of $\text{Ca}_{1-x}\text{Ce}_x\text{MnO}_3$ ($x = 0.167$) at selected temperatures.

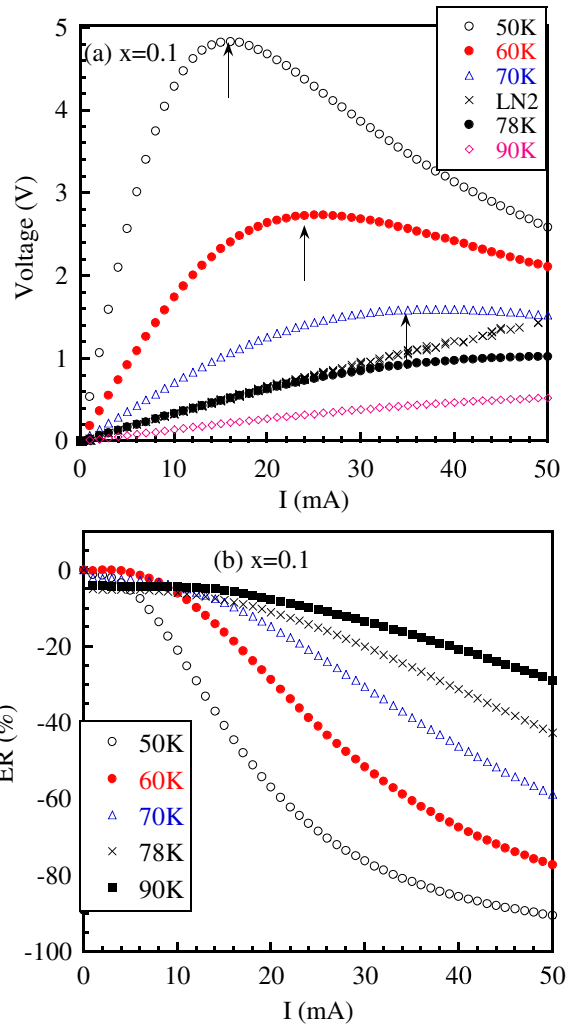


Figure 3. (a) Voltage versus current (VI) characteristics of $\text{Ca}_{1-x}\text{Ce}_x\text{MnO}_3$ ($x = 0.1$) at selected temperatures under a vacuum cryostat. For comparison, we add the IV curve recorded for the sample dipped in liquid nitrogen bath. The arrows indicate threshold currents. A negative differential resistance ($dV/dI < 0$) is observed when the applied current exceeds the threshold value. (b) ER of the $x = 0.1$ sample as a function of applied current.

At the lowest temperature of 70 K, a strong NDR appears even at low currents applied over a threshold value of 5 mA and the application of the high currents up to 50 mA results in a very huge decrease in R by more than one order of magnitude. The corresponding ER attains -98% at $I = 50$ mA. For $x = 0.167$, we obtain $\Delta T = \sim 8$ K ($I = 50$ mA) at 70 K but it does not explain such a huge decrease in R . We expect from figure 1(a) that a temperature rise due to Joule heating suppresses the value of ρ from $840 \Omega \text{ cm}$ at 70 K down to $260 \Omega \text{ cm}$ at 78 K, giving a gradual drop in R by a factor of about one-third. To examine the difference in the thermal environment of the sample in a vacuum cryostat and a liquid N_2 bath, the IV data of the sample immersed in liquid N_2 are given in figure 4(a). In the liquid N_2 bath, we have both a negative differential resistance and its associated huge decrease in R , giving a CER effect achieving ER $= -85\%$ at $I = 50$ mA. The corresponding temperature rise is $\Delta T = \sim 3$ K at $I = 50$ mA for $x = 0.167$ (for $x = 0.1$, ΔT is negligible). It is evident that the effect of Joule heating is not responsible for the huge decrease in R .

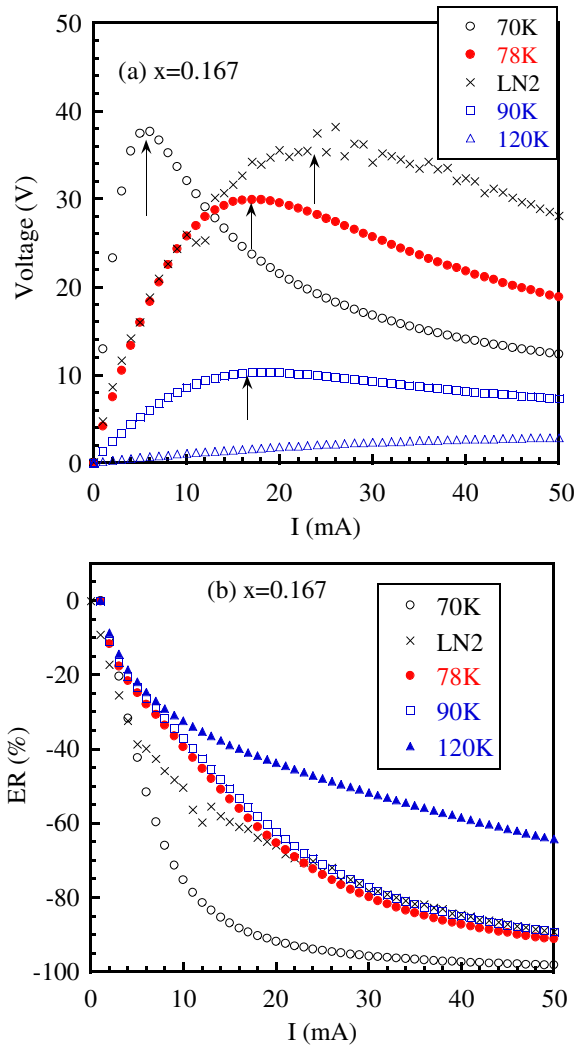


Figure 4. (a) Voltage versus current (VI) characteristics and (b) ER ratio of $\text{Ca}_{1-x}\text{Ce}_x\text{MnO}_3$ ($x = 0.167$) at selected temperatures.

It has been reported that the CO state of the $x = 0.167$ sample is stable in comparison with that of $x = 0.1$ because the concentration of magnetic frustrated bonds decreases with increasing Mn^{3+} ions [20]. In addition, the fraction of CO phase in the $x = 0.1$ sample is estimated to be at most 30% with a majority (70%) of the C-type AFM phase at 12 K, while for the $x = 0.167$ sample it reaches about 80%, suggesting a major fraction of the CO phase. We thus believe that the application of a stronger electric field is needed to transform the stable CO phase into a low resistive state.

Here, we assume that CO clusters are pinned to the lattice through the Jahn–Teller effect of Mn^{3+} ions as pointed out in [21]. We then understand that they are depinned by the application of a strong electric field, resulting in the nonlinear ER effect. Moreover, upon increasing T , a thermally activated depinning becomes more dominant, leading to a smaller ER effect [4]. This pinning model qualitatively describes the giant ER effect enhanced at low T . As for the ER effect in the ferromagnetic insulating phase of $\text{La}_{0.82}\text{Ca}_{0.18}\text{MnO}_3$, the authors argue that the electric current enhances transfer integral between e_g orbitals of neighbouring Mn sites, i.e. increases the e_g bandwidth, which results in a resistance drop [6]. To

our knowledge, we have no experimental evidence for the enhanced bandwidth effect due to the application of a strong electric field on manganites.

4. Summary

We have investigated the nonlinear VI characteristics in a charge-ordered phase of two-electron doped manganites $\text{Ca}_{1-x}\text{Ce}_x\text{MnO}_3$ ($x = 0.1$ and 0.167). The substitution of Ce^{4+} ion for Ca^{2+} site produces two-electron doping with the chemical formula $\text{Ca}_{1-x}^{2+}\text{Ce}_x^{4+}\text{Mn}_{1-2x}^{4+}\text{Mn}_{2x}^{3+}\text{O}_3$. It is pointed out that the Seebeck coefficient data of $\text{Ca}_{0.9}\text{Ce}_{0.1}\text{MnO}_3$ are very similar to those of $\text{Ca}_{0.8}\text{Sm}_{0.2}\text{MnO}_3$, indicating additional evidence for the two-electron doping. We demonstrate that a temperature rise across the samples is not responsible for the huge decrease in R . The VI characteristics measured using a long pulsed current show a negative differential resistance and concomitant giant electroresistance effect. The larger ER effect enhanced for the $x = 0.167$ sample is probably attributed to its stable CO state.

Acknowledgments

This work was partially supported by a Grant-in-Aid for Scientific Research from the Japan Society of the Promotion of Science. The authors thank A Tamura for his technical support.

References

- [1] Tokura Y (ed) 2000 *Colossal Magnetoresistive Oxides* (New York: Gordon and Breach)
- [2] Dagotto E (ed) 2003 *Nanoscale Phase Separation and Colossal Magnetoresistance* (Berlin: Springer)
- [3] Asamitsu A, Tomioka Y, Kuwahara H and Tokura Y 1997 *Nature* **388** 50
- [4] Rao C N R, Raju A R, Ponnambalam V, Parashar S and Kumar N 2000 *Phys. Rev. B* **61** 594
- [5] Markovich V, Rozenberg E, Yuzhelevski Y, Jung G, Gorodetsky G, Shulyatev D A and Mukovskii Ya M 2001 *Appl. Phys. Lett.* **78** 3499
- [6] Mercone S, Wahl A, Simon Ch and Martin C 2002 *Phys. Rev. B* **65** 214428
- [7] Sudheendra L and Rao C N R 2003 *J. Appl. Phys.* **94** 2767
- [8] Odagawa A, Sato H, Inoue I H, Akoh H, Kawasaki M and Tokura Y 2004 *Phys. Rev. B* **70** 224403
- [9] Ma Y Q, Song W H, Dai J M, Zhang R L, Yang J, Zhao B C, Sheng Z G, Lu W J, Du J J and Sun Y P 2004 *Phys. Rev. B* **70** 054413
- [10] Biskup N and de Andres A 2006 *Phys. Rev. B* **74** 184403
- [11] Jain H, Raychaudhuri A K, Mukovski Ya M and Shulyatev D 2006 *Appl. Phys. Lett.* **89** 152116
- [12] Yamato Y, Matsukawa M, Murano Y, Suryanarayanan R, Nimori S, Apostu M, Revcolevschi A, Koyama K and Kobayashi N 2009 *Appl. Phys. Lett.* **94** 092507
- [13] de Andres A, Biskup N, Garcia-Hernandez M and Mukovskii Y M 2009 *Phys. Rev. B* **79** 014437
- [14] Lu W J, Sun Y P, Zhao B C, Zhu X B and Song W H 2006 *Solid State Commun.* **137** 288
- [15] Bose E, Chan C L, Yang H D and Chaudhuri B K 2008 *J. Phys. D: Appl. Phys.* **41** 225005
- [16] Maignan A, Martin C, Damay F and Raveau B 1998 *Chem. Mater.* **10** 950

- [17] Zeng Z, Greenblatt M and Croft M 2001 *Phys. Rev. B* **63** 224410
- [18] Melo Jorge M E, Nunes M R, Maria R S and Sousa D 2005 *Chem. Mater.* **17** 2069
- [19] Hejtmanek J, Jirak Z, Marysko M, Matin C, Maignan A, Hervieu M and Raveau B 1999 *Phys. Rev. B* **60** 14057
- [20] Caspi E N, Avdeev M, Short S, Jorgensen J D, Lobanov M V, Zeng Z, Greenblatt M, Thiyagarajan P, Botez C E and Stephens P W 2004 *Phys. Rev. B* **69** 104402
- [21] Guha A, Ghosh A, Raychaudhuri A K, Parashar S, Raju A R and Rao C N R 1999 *Appl. Phys. Lett.* **75** 3381